Breakdown characteristics of AlGaN/GaN Schottky barrier diodes fabricated on a silicon substrate*

Jiang Chao(蒋 超), Lu Hai(陆 海)†, Chen Dun-Jun(陈敦军), Ren Fang-Fang(任芳芳), Zhang Rong(张 荣), and Zheng You-Dou(郑有炓)

Jiangsu Provincial Key Laboratory of Advanced Photonic and Electronic Materials, and School of Electronic Science and Engineering, Nanjing University, Nanjing 210093, *China*

(Received 20 January 2014; revised manuscript received 26 March 2014; published online 9 July 2014)

In this work, the breakdown characteristics of AlGaN/GaN planar Schottky barrier diodes (SBDs) fabricated on the silicon substrate are investigated. The breakdown voltage (BV) of the SBDs first increases as a function of the anode-to-cathode distance and then tends to saturate at larger inter-electrode spacing. The saturation behavior of the BV is likely caused by the vertical breakdown through the intrinsic GaN buffer layer on silicon, which is supported by the post-breakdown primary leakage path analysis with the emission microscopy. Surface passivation and field plate termination are found effective to suppress the leakage current and enhance the BV of the SBDs. A high BV of 601 V is obtained with a low on-resistance of 3.15 mΩ·cm^2.

Keywords: AlGaN/GaN, Schottky barrier diodes, silicon substrate, breakdown

PACS: 73.61.Ey, 73.40.Kp, 85.30.Kk **DOI:** 10.1088/1674-1056/23/9/097308

1. Introduction

GaN is one of the most promising candidate materials for power electronic applications due to its superior material characteristics such as large bandgap, high breakdown electrical field, high electron saturation velocity, and the ability to form hetero-junctions with other III-nitride materials.[1–3] Recently, GaN grown on the silicon substrate has drawn much attention.[4–6] Compared with the conventional sapphire substrate, the high thermal conductivity of silicon is highly desirable for power device applications. Meanwhile, a high-quality Si substrate with a large diameter can be easily obtained at low cost. However, the growth of GaN on Si is difficult due to the large lattice and thermal mismatch between the two materials. As a result, sophisticated and optimized buffer structures have to be developed for growing a high quality GaN epilayer on Si.[7,8]

A key performance parameter of the GaN-based power devices is the maximum reverse breakdown voltage (BV), which not only depends on the material quality of the active layers, but also relies on the specific termination and passivation techniques applied.[9–12] For the case of GaN on Si, the situation is more complex as Si normally has a high conductivity and the critical electrical field of Si is much smaller than that of GaN. It is expected that the Si substrate could be the limiting factor for the maximum BVs of the GaN-on-Si power devices, which is evidenced by the enhanced BVs of AlGaN/GaN-on-Si high-electron-mobility transistors (HEMTs) after the removal of the Si substrates.[13,14] In addition, it was also reported that the BVs of AlGaN/GaN-on-Si HEMTs can be improved by using a thicker buffer layer.[8] Although some promising results of GaN-on-Si power devices have been reported, it is clear that the technology is still in its early development stage. Nowadays, GaN-on-Si power devices often exhibit high leakage currents and premature breakdown and the question what exactly is responsible for the high leakage current and low breakdown voltage remains unanswered in many practical situations.

In this work, AlGaN/GaN Schottky barrier diodes (SBDs) are grown and fabricated on the Si substrate to investigate their breakdown-related behavior and potential power device performance. Emission microscopy (EMMI) is firstly employed to study the primary leakage path after the hard breakdown, which is effective to reveal the exact breakdown location.[15,16] Detailed breakdown mechanisms are discussed. The effects of the surface passivation and the field-plate termination are also studied to improve the breakdown characteristics of the GaN-based SBDs on Si.

2. Device structure and fabrication

The epi-structure used in this work is grown on a (111) Si substrate by metal-organic chemical vapor deposition, which consists of an AlN nucleation layer, an AlGaN/GaN superlattice strain-relief layer, a 2-μm undoped GaN buffer layer, and a 25-nm undoped $Al_{0.2}Ga_{0.8}N$ barrier layer. Based on

*Project supported by the National Basic Research Program of China (Grant Nos. 2010CB327504, 2011CB922100, and 2011CB301900), the National Natural Science Foundation of China (Grant Nos. 60936004 and 11104130), the Natural Science Foundation of Jiangsu Province, China (Grant Nos. BK2011556 and BK2011050), and the Priority Academic Development Program of Jiangsu Higher Education Institutions, China.

†Corresponding author. E-mail: hailu@nju.edu.cn

© 2014 Chinese Physical Society and IOP Publishing Ltd

the capacitance–voltage (C–V) measurement, the calculated 2-dimensional electron gas (2DEG) density of the heterostructure is about 4.32×10^{12} cm^{-2} (Fig. 1). The diode structure consists of 110 μm circular Schottky dots separated radially from the Ohmic contacts. The inter spacing between the two electrodes varies from 5 μm to 100 μm. The Ohmic contacts are formed by rapid thermal annealing a Ti/Al/Ti/Au (30 nm/80 nm/30 nm/100 nm) metal stack at 850 °C for 30 s in an N_2 environment. The lift-off technique is used to pattern the Ni/Au (200 nm/50 nm) based Schottky contact dots. The SBDs are either unpassivated or passivated by 200 nm SiO_2 deposited by plasma enhanced chemical vapor deposition. For the comparative study, some passivated devices are further terminated by field plates with an edge overlap of 2 μm. Figure 2 shows the cross-sectional schematics of the various devices fabricated as well as a top view image of one selected device chip.

The current–voltage (I–V) characteristics of the SBDs with the substrate floating are measured by using a Keithley 237 high-voltage source-measure unit. To avoid surface flashover, the device under test is immersed in a Fluorinert fluid. For each device configuration, 20 identical devices are randomly chosen and measured for evaluating the device performance statistically. The EMMI analysis is conducted to locate the exact breakdown spots of some post-breakdown devices. During the EMMI measurement, the SBD is biased at −5 V and the integration time for collecting the photoemission image is set to be 5 min.

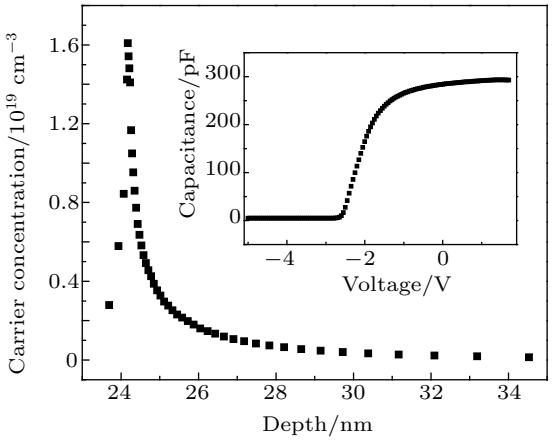


Fig. 1. Distribution of the 2DEG density as a function of depth calculated from the C–V measurement. The inset shows the original C–V curve of the epitaxial layer measured by using a Hg probe with a Schottky contact diameter of 0.46 mm.

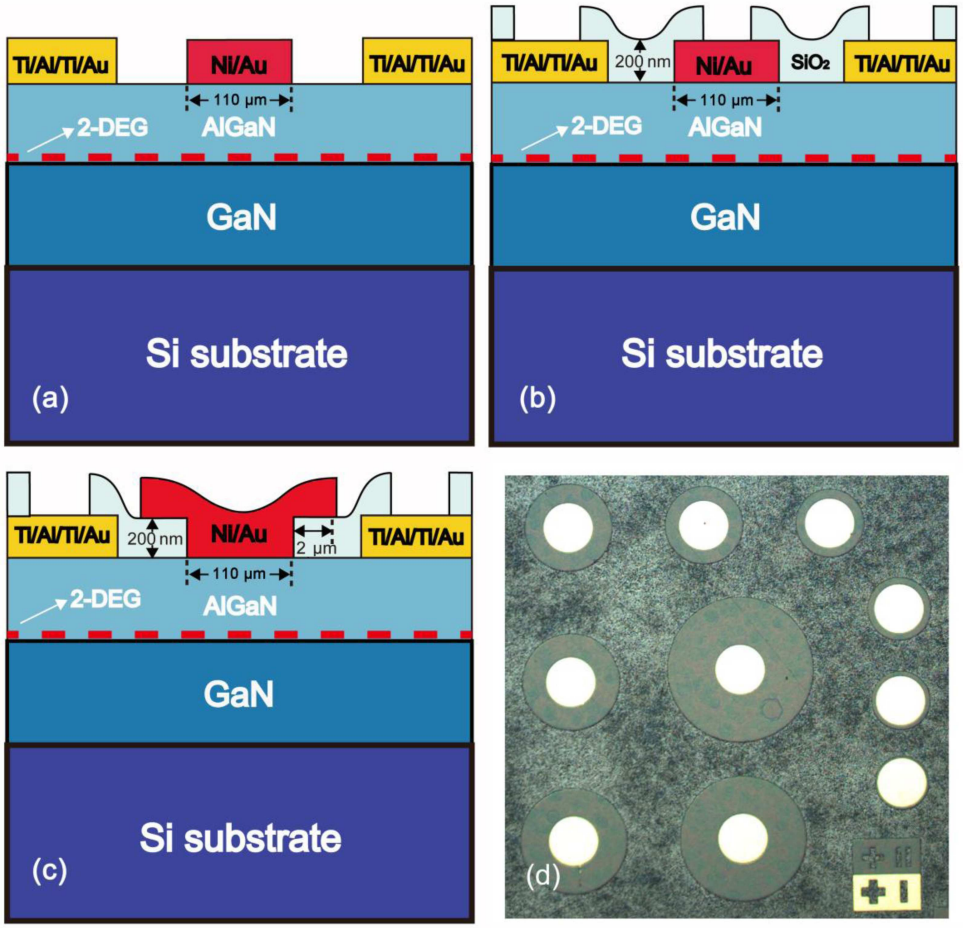


Fig. 2. (color online) Schematic diagrams of various AlGaN/GaN planar SBDs fabricated on the Si substrate: (a) bare device; (b) device with surface passivation; (c) device with surface passivation and field-plate termination; (d) top-view photograph of a fabricated chip.

3. Results and discussion

The BVs of the SBDs with and without surface passivation are shown in Fig. 3(a) as a function of the Schottky-to-Ohmic spacing L_s. It is clear that the BVs of the SBDs first rise as L_s increases, and then tend to saturate at larger L_s (> 20 μm). This observation is quite different from that of the AlGaN/GaN-based SBDs fabricated on the sapphire substrate, in which no saturation of BVs could be observed.[17] Meanwhile, the BVs of the passivated devices are always higher than those of the unpassivated devices and the difference becomes small for the devices with large L_s. Figure 3(b) shows the typical reverse I–V characteristics of four selected types of devices. It is found that the enhancement of the SBDs upon passivation is correlated with the reduction of the leakage current at a lower reverse bias.

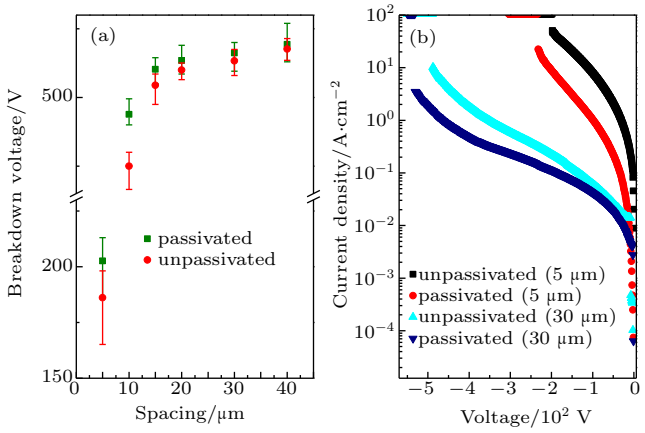


Fig. 3. (color online) (a) BVs of passivated and unpassivated SBDs as a function of the contact spacing. The upper and the lower limits of the obtained BVs as well as the average value of the BVs are shown by the error bars and the inner solid mark, respectively. (b) Typical reverse I–V characteristics of unpassivated and passivated SBDs.

According to the past off-state breakdown study of AlGaN/GaN HEMTs grown on Si, the increase of BVs as a function of L_s at the lower L_s range is likely caused by the horizontal breakdown across the semiconductor surface, while the saturation of BVs at higher L_s is likely due to the vertical breakdown through the GaN buffer layer.[18] More specifically, due to the field crowding effect, there is always an electrical field spike along the edge of the Schottky contact. The magnitude and the profile of the electrical field spike are affected by many factors, including the electrode spacing, the specific termination structure, and the conductivity of the floating substrate. Besides directly reducing the parasitic surface leakage, the surface passivation may also affect the field distribution to a certain degree by passivating the surface defects near the contact edge. Since the primary leakage current from the AlGaN/GaN-based Schottky contacts is strongly field-dependent, which could be based on either thermionic field emission[18,19] or Frenkel–Poole emission,[20] it is not surprising that the final BVs obtained have a strong correlation with the magnitude of the leakage current.

For the case of SBDs with small L_s, the horizontal component of the edge electrical field is strong, leading to relatively small BVs. As L_s increases, due to the field spreading effect, the peak horizontal field component becomes relatively smaller at the same reverse bias. As a result, a higher BV can be obtained at a larger L_s. However, when L_s is sufficiently large (e.g., larger than 20 μm in the present case), the vertical component of the edge electrical field could become a dominant factor determining the electrical breakdown. This situation is particularly true when the device is fabricated on a low resistivity substrate like Si. It is believed that the main effect of the Si substrate is to electrical-statically modify the electrical field profile and strengthen the overall vertical field component. Therefore, the vertical breakdown should still first initiate at the GaN surface along the contact edge and the resulting conduction path would extend vertically down to the Si substrate. Based on this argument, although Si indeed has a much lower breakdown electrical field than that of GaN, what really matters is the conductivity of the Si substrate, and the breakdown through the GaN buffer probably proceeds that at the GaN/Si interface under a high reverse bias.

The EMMI measurement along with optical microscopy is used to investigate the above physical analysis. It is found that after the forced breakdown, although the SBDs still exhibit a rectification behavior, a very high reverse leakage current is observed in these devices. The leakage current preferentially flows through the breakdown paths, which would create localized hot spots. Figure 4 shows the EMMI images as well as the corresponding conventional optical images of two selected post-breakdown devices with $L_s = 10$ μm and 40 μm. For the $L_s = 10$ μm device, a string of hot spots are observed on the GaN surface extending from the Schottky metal to the Ohmic metal. A patch of burn mark appears around the same location in the conventional optical image, which is caused by excessive local heating during the breakdown. Thus, the EMMI result agrees with the physical picture of horizontal breakdown at small electrode spacing. The exact location of the breakdown point around the circular Schottky contact is determined by the local defect density and the relative sharpness of the metal edge. Meanwhile, for the $L_s = 40$ μm device, a single hot spot is observed at the Schottky contact edge, which stays within a crater created by the breakdown-induced crystalline damage. Typically, some radial channels can be observed around the crater. However, no hot spot appears along with these channels as shown in the EMMI image. This observation verifies the suggested vertical breakdown phenomenon.

Furthermore, besides an appropriate surface passivation, a field plate termination can also effectively enhance the BVs of the SBDs. As shown in Fig. 5(b), the reverse leakage cur-

rent is considerably suppressed when the field plate termination is employed for both small L_s and large L_s devices, meaning that the peak electrical field along the Schottky contact edge is reduced. The BVs of the SBDs are enhanced simultaneously. In addition, the apparent BV improvement at larger L_s supports the point that the vertical breakdown initiates at the GaN surface instead of the GaN/Si interface, as the field plate mostly modifies the profile of the surface electrical field.[21]

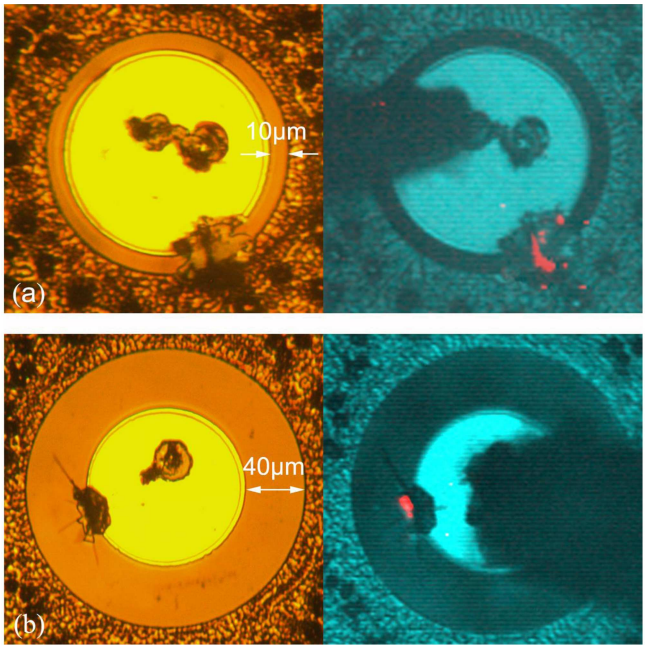


Fig. 4. (color online) The EMMI images (right) as well as the corresponding conventional optical images (left) of two selected post-breakdown devices with $L_s = 10$ μm (a) and 40 μm (b).

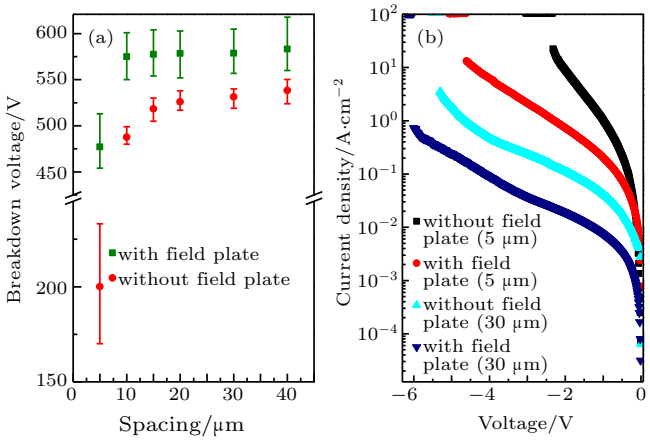


Fig. 5. (color online) (a) BVs of the SBDs with and without field plate termination as a function of the contact spacing. The upper and the lower limits of the obtained BVs as well as the average value of the BVs are shown by the error bars and the inner solid mark, respectively. (b) Typical reverse *I*–*V* characteristics of the SBDs with and without field plate termination.

The forward *I*–*V* curves as well as the corresponding on-resistances of the field plate-terminated SBDs with various L_s are shown in Fig. 6. The on-resistance increases nearly linearly as a function of L_s. A sheet resistance of 1142 Ω/□ for the 2DEG conductive channel is deduced from the slope of the on-resistance versus L_s plot. It is found that when $L_s = 10$ μm, a maximum BV of 601 V can be obtained in this work with on-resistance $R_{ON} = 3.15$ mΩ·cm^2.

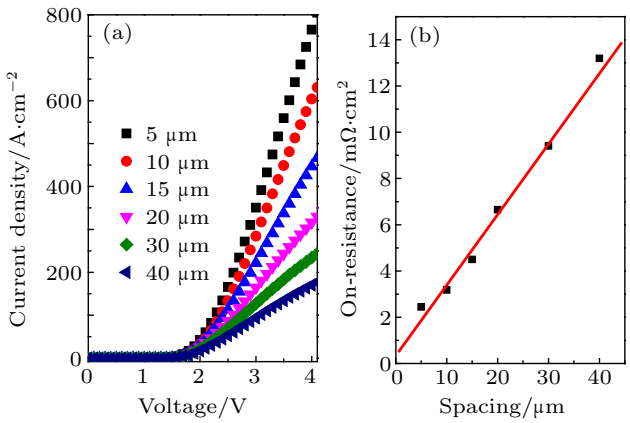


Fig. 6. (color online) (a) Typical forward *I*–*V* characteristics of the field-plate-terminated SBDs with various contact spacings; (b) the corresponding on-resistances of the SBDs calculated as function of the contact spacing.

4. Conclusion

The breakdown characteristics of AlGaN/GaN-based planar SBDs fabricated on the Si substrate are investigated in this work. It is found that the BV of the SBDs increases as a function of L_s in the low L_s range and then tends to saturate at larger L_s, which are due to the horizontal and the vertical breakdowns, respectively. The breakdown modes are supported by our EMMI analysis, which reveals the primary leakage paths in the SBDs after the hard breakdown. Surface passivation and field plate termination are found effective to suppress the leakage current and enhance the BV of the SBDs. A low on-resistance (R_{ON}) of 3.15 mΩ·cm^2 is obtained with a high BV of more than 600 V. It is further suggested that the high conductivity of the Si substrate is the primary factor inducing the vertical breakdown through the GaN buffer, which electrical-statically modifies the electrical field profile and strengthens the overall vertical field component.

References

[1] Jain S C, Willander M, Narayan J and Overstraeten R V 2000 *J. Appl. Phys.* **87** 965
[2] Nishikawa A, Kumakura K, Akasaka T and Makimoto T 2006 *Appl. Phys. Lett.* **88** 173508
[3] Cao XA, Lu H, LeBoeuf S F, Cowen C, Arthur S D and Wang W 2005 *Appl. Phys. Lett.* **87** 053503
[4] Lu B and Palacios T 2010 *IEEE Electron Device Lett.* **31** 951
[5] Selvaraj S L, Watanabe A, Wakejima A and Egawa T 2012 *IEEE Electron Device Lett.* **33** 1375
[6] Xia L, Hanson A, Boles T and Jin D H 2013 *Appl. Phys. Lett.* **102** 113510
[7] Ikeda N, Niiyama Y, Kambayashi H, Sato Y, Nomura T, Kato S and Yoshida S 2010 *Proc. IEEE* **98** 1151
[8] Kato S, Satoh Y, Sasaki H, Masayuki I and Yoshida S 2007 *J. Cryst. Growth* **298** 831
[9] Green B M, Chu K K, Chumbes E M, Smart J A, Shealy J R and Eastman L F 2000 *IEEE Electron Device Lett.* **21** 268
[10] Tarplee M C, Madangarli V P, Zhang Q and Sudarshan T S 2001 *IEEE Trans. Electron Devices* **48** 2659

[11] Saxena V, Su J N and Steckl A J 1999 *IEEE Trans. Electron Devices* **46** 456
[12] Wu Y F, Saxler A Moore M Smith R P, Sheppard S, Chavarkar P M, Wisleder T, Mishra U K and Parikh P 2004 *IEEE Electron Device Lett.* **25** 117
[13] Srivastava P, Das J, Visalli D, Derluyn J, Hove M V, Malinowski P E, Marcon D, Geens K, Cheng K, Degroote S, Leys M, Germain M, Decoutere S, Mertens R P and Borghs G 2010 *IEEE Electron Device Lett.* **31** 851
[14] Visalli D, Hove M V, Derluyn J, Srivastava P, Marcon D, Das J, Leys M R, Degroote S, Cheng K, Vandenplas E, Germain M and Borghs G 2010 *IEEE Trans. Electron Devices* **57** 3333
[15] Chynoweth A G and McKay K G 1956 *Phys. Rev.* **102** 369
[16] Kölzer J, Boit C, Dallmann A, Deboy G, Otto J and Weinmann D 1992 *J. Appl. Phys.* **71** R23
[17] Cao D S, Lu H, Chen D J, Han P, Zhang R and Zheng Y D 2011 *Chin. Phys. Lett.* **28** 017303
[18] Miller E J, Dang X Z and Yu E T 2000 *J. Appl. Phys.* **88** 5951
[19] Hashizume T, Kotani J and Hasegawa H 2004 *Appl. Phys. Lett.* **84** 4884
[20] Yan DW, Lu H, Cao D S, Chen D J, Zhang R and Zheng Y D 2010 *Appl. Phys. Lett.* **97** 153503
[21] Karmalkar S and Mishra U K 2001 *IEEE Trans. Electron Devices* **48** 1515